

# Typical versus average helicity modulus in the three-dimensional gauge glass: Understanding the vortex glass phase

Helmut G. Katzgraber, D. Würtz, and G. Blatter  
*Theoretische Physik, ETH Zürich, CH-8093 Zürich, Switzerland*  
 (Dated: June 19, 2021)

We numerically compute the helicity modulus of the three-dimensional gauge glass by Monte Carlo simulations. Because the average free energy is independent of a twist angle, it is expected that the average helicity modulus, directly related to the superfluid density, vanishes when simulations are performed with periodic boundary conditions. This is not necessarily the case for the typical (median) value, which is nonzero, because the distribution of the helicity modulus among different disorder realizations is very asymmetric. We show that the data for the helicity modulus distribution are well described by a generalized extreme-value distribution with a nonzero location parameter (most probable value). A finite-size scaling analysis of the location parameter yields a critical temperature and critical exponents in agreement with previous results. This suggests that the location parameter is a good observable. There have been conflicting claims as to whether the superfluid density vanishes in the vortex glass phase, with Fisher *et al.* [Phys. Rev. B **43**, 130 (1991)] arguing that it is finite and Korshunov [Phys. Rev. B **63**, 174514 (2001)] predicting that it is zero. Because the gauge glass is commonly used to describe the vortex glass in high-temperature superconductors, we discuss this issue in light of our results on the gauge glass.

PACS numbers: 75.50.Lk, 75.40.Mg, 05.50.+q

## I. INTRODUCTION

The gauge glass is often used to describe the extremely disordered vortex glass phase in granular high-temperature superconductors.<sup>1,2,3,4</sup> In addition, it is the simplest possible model that possesses the correct order parameter symmetry [ $XY$  spins with a  $U(1)$  symmetry] and therefore considerable numerical, as well as theoretical, work has been based on it. Nevertheless, the model has some limitations: it is isotropic, whereas finite magnetic fields in the vortex glass phase in high-temperature superconductors introduce a uniaxial field anisotropy.<sup>5</sup> Furthermore, the gauge glass ignores transverse screening, an essential ingredient in superconductivity. In fact, the inclusion of screening destroys the gauge glass phase and the critical temperature drops to zero.<sup>6</sup> In addition, the disorder is introduced via random gauge fields, whereas a more realistic model would probably introduce the disorder via random bonds.<sup>7,8</sup>

In three space dimensions the (unscreened) gauge glass undergoes a phase transition into a glassy phase at  $T_c = 0.47(3)$ ,<sup>11</sup> which has been estimated by a finite-size scaling analysis of the currents in the system (first-order derivative of the free energy with respect to an infinitesimal twist to the boundaries).<sup>11</sup> Another central quantity to study is the helicity modulus—directly related to the superfluid density—which corresponds to the second-order derivative of the free energy with respect to an infinitesimal twist to the boundaries. Motivated by contradicting predictions as to whether the superfluid density  $\rho_s$  is finite or not for a bulk vortex glass system,<sup>12,13</sup> we have studied in detail the helicity modulus of the three-dimensional gauge glass model. Because the simulations are performed using periodic boundary conditions in order to avoid finite-size effects due to small system sizes,

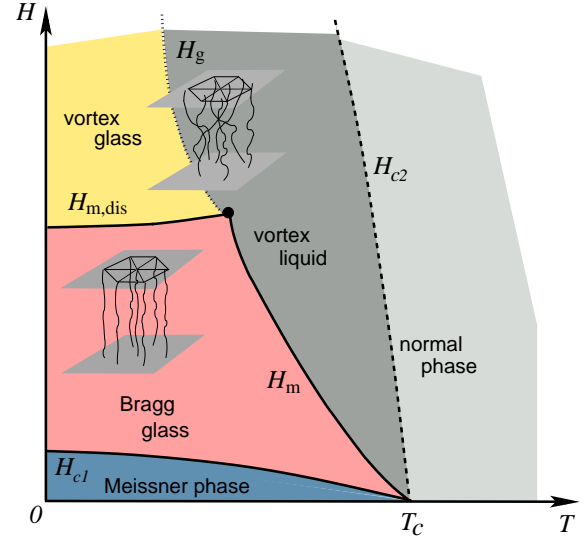


FIG. 1: (Color online) Possible phase diagram of a disordered superconductor (Ref. 4). The vortex lines are pinned by defects and the vortex solid found in a clean superconductor is transformed into a glass. For low disorder, there are no dislocations and one obtains a Bragg glass which exhibits a superconducting response, whereas for high disorder and low enough, temperatures a highly disordered vortex glass phase emerges (Ref. 9). The vortex liquid remains liquid after the inclusion of disorder, albeit viscous and separated by a glass transition line  $H_g$  (dotted line) from the vortex glass phase.  $H_{c1}$  separates the Bragg glass phase from the Meissner phase, whereas  $H_{c2}$  denotes the crossover from the superconducting to the normal phase (Ref. 10) (mean-field calculation, dashed line). The melting lines between Bragg glass, vortex glass, and vortex liquid are denoted by  $H_m$  and are calculated taking into account fluctuations. (Figure adapted from Ref. 4).

we expect that the average of the helicity modulus is zero. This (unphysical) result follows from twists forced into the system due to the used periodic boundary conditions. The problem can be alleviated by using either free boundary conditions or fluctuating-twist boundary conditions,<sup>14,15</sup> where location-dependent twists are applied along the boundaries. The former have the problem that corrections to scaling are huge for numerically accessible system sizes and the latter generally overestimate the stiffness of the system.

Our results with periodic boundary conditions show that the mean of the helicity modulus does not have critical scaling, thus preventing us from determining the location of the glass transition. In addition, strong fluctuations in the mean develop below the transition temperature. In contrast, the typical (median) value shows the correct scaling, i.e., the data cross at the known value of the transition temperature. Furthermore, we demonstrate that the data are well fitted by extreme-value distributions, commonly used in economics studies,<sup>16,17,18</sup> explaining the strong fluctuations in the mean as well as providing detailed estimates of the critical parameters via a finite-size scaling analysis of the location parameter of the helicity modulus distributions (most probable value).

The gauge glass has attracted interest in the context of disordered high-temperature superconductors. The phase diagram of such disordered type-II materials exhibits numerous phases<sup>1,2,3,4</sup> (see Fig. 1) and, despite intensive research, several features of the different phase diagrams of high-temperature superconductors in a magnetic field remain to be fully understood. In the presence of disorder the Abrikosov lattice ceases to be perfect. For low enough temperatures and fields (above  $H_{c1}$ ), a Bragg glass emerges<sup>4</sup> characterized by the appearance of algebraic Bragg peaks when spectroscopic measurements are performed, even though the flux line lattice is disordered. These are lost when either the disorder or the temperature is increased. Increasing the temperature yields a vortex liquid, where flux lines fluctuate subject to a random disorder potential. Increasing the disorder yields a vortex glass phase<sup>9,19</sup> where the order of the flux line lattice is destroyed and the vortex lines are strongly pinned to the impurities with no spatial order – similar to standard spin glasses<sup>20</sup> (see Fig. 1). Signatures of a vortex glass phase have been observed experimentally by studying the  $I$ - $V$  characteristics of YBCO samples. There the vanishing of the resistivity for fields larger than  $H_{c1}$  has been interpreted as the onset of a vortex glass phase.<sup>21,22,23</sup> Furthermore, a recent microscopic study<sup>24</sup> on LSCO samples using muon-spin rotation experiments and small-angle neutron scattering shows the transition from a Bragg to a vortex glass phase.

Fisher *et al.*<sup>12</sup> argue that the superfluid density  $\rho_s$  is finite in the thermodynamic limit, with finite-frequency corrections that only vanish as an inverse power of  $\ln(\omega)$ . In contrast, Korshunov<sup>13</sup> recently predicted that the superfluid density tends to *zero* logarithmically in  $\omega$ . Be-

cause the superfluid density can be directly related to the helicity modulus, it is tempting to describe the strongly disordered vortex glass phase by numerically studying the gauge glass model, although certain aforementioned provisions need to be considered: the gauge glass model does not include a field anisotropy and it does not have transverse screening. We use our results for the helicity modulus in the gauge glass to discuss the superfluid density in the vortex glass, and thus, test if the superfluid density vanishes in the thermodynamic limit or if it stays finite when the system is in *equilibrium* ( $\omega = 0$ ). Our results from equilibrium Monte Carlo simulations of the gauge glass for the helicity modulus show that for the system sizes studied the superfluid density remains finite in the thermodynamic limit.

The paper is structured as follows: In Sec. II we introduce the model, observables, and the numerical method used. In Sec. III we present our results, followed by concluding remarks in Sec. IV.

## II. MODEL, OBSERVABLES, AND NUMERICAL DETAILS

The Hamiltonian of the gauge glass is given by

$$\mathcal{H} = - \sum_{\langle i,j \rangle} J_{ij} \cos(\phi_i - \phi_j - A_{ij}), \quad (1)$$

where the sum ranges over nearest neighbors on a cubic lattice in three space dimensions of size  $N = L^3$ , and  $\phi_i$  represent the angles of the  $XY$  spins. For the gauge glass,  $J_{ij} = J \forall i, j$  in Eq. (1) and in this work we set  $J = 1$ . Periodic boundary conditions (PBCs) are applied. The  $A_{ij}$  represents the line integral of the vector potential between sites  $i$  and  $j$ , and we chose the  $A_{ij}$  from a uniform distribution in  $[0, 2\pi]$  but with the constraint that  $A_{ij} = -A_{ji}$ .<sup>25</sup> In three space dimensions, the model exhibits a finite-temperature spin-glass transition<sup>11</sup> at  $T_c \approx 0.47 \pm 0.03$ . Note that when screening is added to the Hamiltonian in Eq. (1), the transition to a glass phase is lost.<sup>6</sup>

The helicity modulus  $Y$  is the second-order derivative of the free energy  $F$  with respect to an infinitesimal twist  $\Theta$  to the boundaries,<sup>26</sup> i.e.,  $Y = \partial^2 F / \partial \Theta^2 |_{\Theta \rightarrow 0}$ ,

$$Y = \frac{1}{L^2} \left[ \sum_i \langle \cos(\Delta_i) \rangle - \frac{1}{T} \sum_{i,j} \langle \sin(\Delta_i) \sin(\Delta_j) \rangle - \langle \sin(\Delta_i) \rangle \langle \sin(\Delta_j) \rangle \right]. \quad (2)$$

In Eq. (2),  $\langle \dots \rangle$  represents a thermal average and  $\Delta_i = \phi_i - \phi_{i+x} - A_{ii+x}$ , where the twist is performed along the  $x$  axis.<sup>27</sup> Because a disorder average of the free energy  $F$  is independent of the twist angle, we expect that

$$[Y]_{\text{av}} = 0 \quad (\text{PBC}), \quad (3)$$

where  $[\dots]_{\text{av}}$  represents a disorder average. This is not necessarily the case for the *typical* (median) value  $[Y]_{\text{typ}}$ .

If we study the distribution  $P(Y)$  of  $Y$ , then we expect a large positive contribution due to spin waves. In addition, abrupt changes in the slope of the free energy  $F$  due to sudden vortex rearrangements in certain disorder configurations will generate rare, very negative values of the helicity modulus  $Y$ , thus generating a long negative tail in the distribution<sup>26</sup> (see Fig. 2). This immediately poses the question of whether the different moments of the distribution are properly defined. Especially for low temperatures  $T \ll T_c$ , we expect the tail of the distribution to be most pronounced due to the low probability of vortex rearrangements.

In order to better quantify the effects of the tail of the distribution, we empirically fit the data to a generalized extreme-value distribution,<sup>16,17</sup> which, in general, is the limiting distribution of the maxima of a sequence of independent and identically distributed random variables. Because of this property, generalized extreme-value distributions are used as an approximation to model the maxima of long (finite) sequences of random variables that can be, for example, found in the analysis of stock market data or time series in flat-histogram methods.<sup>28,29</sup> Note that Bertin and Clusel<sup>30</sup> have shown that sums of correlated variables also yield limiting distributions, which can be described by extreme-value distributions. Therefore an underlying extreme process is not necessary to obtain an extreme-value limiting distribution. In addition to the aforementioned applications, extreme-value distributions have recently been used to study different problems in other areas of science ranging from physics and astronomy to biology applications. In the present context, the use of extreme-value distributions is motivated by the extremely skewed shape of the helicity modulus distribution as well as the strong fluctuations found in the mean and the standard deviation.

The cumulative (integrated) generalized extreme-value distribution is given by

$$H_C(x) = \exp \left[ - \left( 1 + \xi \frac{x - \mu}{\beta} \right)^{-1/\xi} \right], \quad (4)$$

where  $\mu$  is the “location parameter” (most probable value),  $\beta$  the “scale parameter” (standard deviation of the peak), and  $\xi$  is the “shape parameter” which indicates the asymptotic behavior of the tail of the distribution. The generalized extreme-value distribution is then given by

$$H(x) = \frac{dH_C(x)}{dx}, \quad (5)$$

where  $H_C(x)$  is given by Eq. (4). In Eq. (5), when  $\xi < 0$  we obtain a thin-tailed (decay faster than exponential) Weibull distribution. If  $\xi = 0$ , we obtain a Gumbel extreme-value distribution (exponential tail), whereas if  $\xi > 0$ , we obtain a fat-tailed Fréchet distribution where the tail falls off slower than an exponential. This has the effect that when  $\xi > 0$ , the  $m$ th moment of the Fréchet distribution exists only if  $\xi < 1/m$ ; i.e., if  $\xi > 1/2$ , the

variance of the distribution is not defined, and if  $\xi > 1$  the mean is not properly defined either. Here, we expect that the distribution of the helicity modulus is well fitted by an extreme-value distribution, i.e.,

$$P(Y) = H(-Y), \quad (6)$$

where  $H(x)$  is given by Eq. (5).

Finally, the superfluid density  $\rho_s$  is related to the helicity modulus via<sup>26</sup>

$$\rho_s = L^{2-d} Y, \quad (7)$$

where  $d$  represents the space dimension. In the present case,  $d = 3$  and thus  $\rho_s = L^{-1} Y$ . Therefore, by investigating the properties of the helicity modulus of the gauge glass, we can also obtain information about the superfluid density of the model.

The simulations are performed using the parallel tempering Monte Carlo method.<sup>31,32</sup> To ensure that the data are in equilibrium, we perform a logarithmic binning of the moments of different observables (such as the currents<sup>11,26,33</sup> and the helicity modulus defined above) and ensure that the data are independent of Monte Carlo steps for the last three bins.<sup>34</sup> In addition, we ensure that the acceptance probabilities for the parallel tempering moves are always greater than 0.3. In order to speed up the simulations, we discretize the angles of the  $XY$  spins to  $N_\phi = 512$  values, a number large enough to avoid crossover effects to other models.<sup>35</sup> Finally, to ensure that the local spin flips are accepted often enough at low temperatures ( $\sim 20\%$ ), we select the proposed new angle for a spin from a temperature-dependent window around the original angle, i.e.,  $\Delta\phi \propto T$  with a minimum angle for low temperatures of  $5^\circ$ . The simulation parameters are presented in Table I. Note that to avoid statistical bias in the computation of the helicity modulus, *four* replicas of the system have been used for each temperature simulated.

The data are fitted to a generalized extreme-value distribution using the statistics package R (see Refs. 18 and 36) using the `fgev` optimization routine in the `evd` package.

### III. RESULTS

Figure 2 shows the distribution of the helicity modulus in the disorder for different system sizes at  $T = 0.409$ , which is below the known value of  $T_c = 0.47(3)$ .<sup>11</sup> The data show a peak for  $Y \gtrsim 0$  and a long tail that extends to large negative values, in agreement with the discussion in Sec. II. The behavior of the tail can be studied in more detail in a semilogarithmic plot, see Fig. 3. For  $T < T_c$ , the tail decays slower than exponential, thus illustrating the possibility of moments of the distribution not being properly defined. In contrast, for  $T > T_c$ , the tail of the distribution decays faster than exponential, as can be seen, for example, for  $T = 0.791$  in Fig. 4.

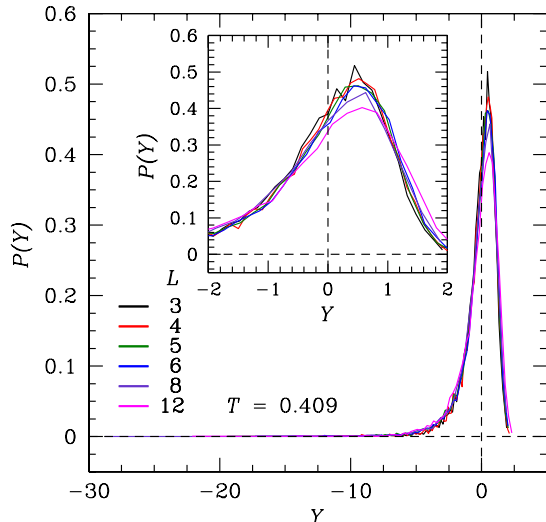


FIG. 2: (Color online) Distribution of the helicity modulus  $P(Y)$  for different system sizes  $L$  at  $T = 0.409 < T_c$ . The data show a pronounced peak close to  $Y \gtrsim 0$  (see inset) and a long tail for  $Y < 0$  which grows with increasing system size, thus suggesting that the data are extreme-value distributed. The dashed lines are guides for the eyes.

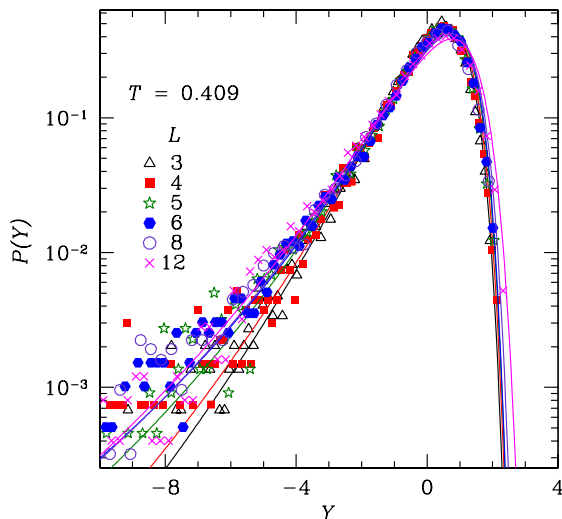


FIG. 3: (Color online) Data for the distribution of the helicity modulus  $P(Y)$  shown in Fig. 2 in a linear-logarithmic plot. The curvature in the tails indicates that the data are Fréchet distributed with a positive shape parameter  $\xi$  for  $T = 0.409 < T_c$ . The width of the tail increases slightly with increasing system size  $L$ . The error bars are not shown for clarity.

TABLE I: Parameters of the simulation.  $N_{sw}$  is the total number of Monte Carlo sweeps,  $T_{min}$  is the lowest temperature simulated, and  $N_T$  is the number of temperatures used in the parallel tempering method (Ref. 37) for each system size  $L$ . The highest temperature simulated is  $T_{max} = 0.947 \gg T_c$ . For each system size,  $N_{sa} = 10^4$  samples have been simulated in order to probe the tails of the distribution in detail.

$L$	$N_{sw}$	$T_{min}$	$N_T$
3	$6.0 \times 10^3$	0.050	53
4	$2.0 \times 10^4$	0.050	53
5	$6.0 \times 10^4$	0.050	53
6	$2.0 \times 10^5$	0.050	53
8	$1.2 \times 10^6$	0.050	53
12	$1.2 \times 10^6$	0.303	38

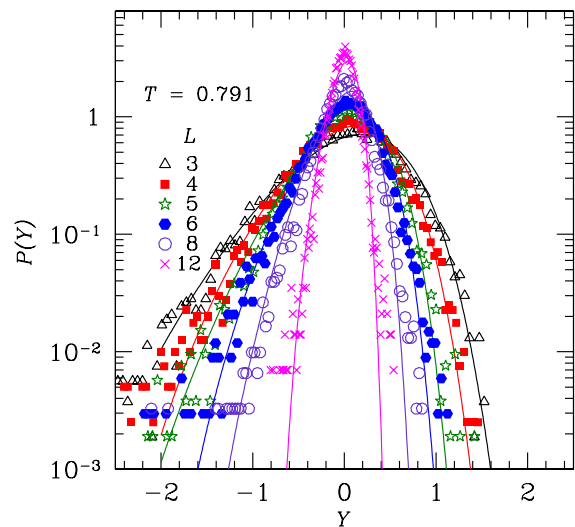


FIG. 4: (Color online) Linear-logarithmic plot of the distribution of the helicity modulus  $P(Y)$  for  $T = 0.791 > T_c$ . The tails of the distribution decay faster than exponential, thus suggesting that the data are well described by a thin-tailed Weibull distribution with  $\xi < 0$ . The error bars are not shown for clarity.

In Fig. 5, we show the average helicity modulus as a function of temperature for different system sizes. Following previous arguments, we expect  $[Y]_{av} = 0$ . This is the case for high enough temperatures, yet for low temperatures the data fluctuate strongly with increasing system size due to the thick tails of the distributions, even for a large number of disorder realizations. Because we expect  $[Y]_{av} = 0$ , the data show no evidence of the phase transition; i.e., there is no crossing of the data for different system sizes as one would expect from a finite-size scaling analysis. This is not the case for the typical value (median) of the distribution (Fig. 6), where the data are clearly nonzero and cross approximately at the known

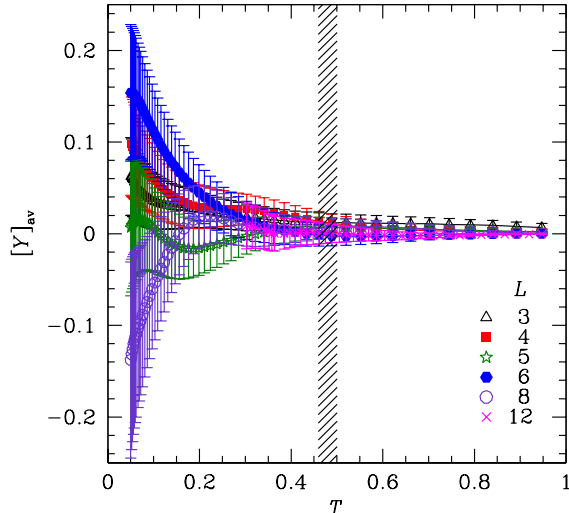


FIG. 5: (Color online) Average helicity modulus  $[Y]_{\text{ave}}$  as a function of temperature for several system sizes. The average should be zero within error bars for all temperatures. The data show that this is the case for  $T > T_c$ , whereas for  $T < T_c$ , due to the fat tails of the distributions (see Fig. 2), the fluctuations in the mean as well as the standard deviation are extremely large. Note that the data show no signature of the phase transition at  $T_c \approx 0.47$  (shaded area).

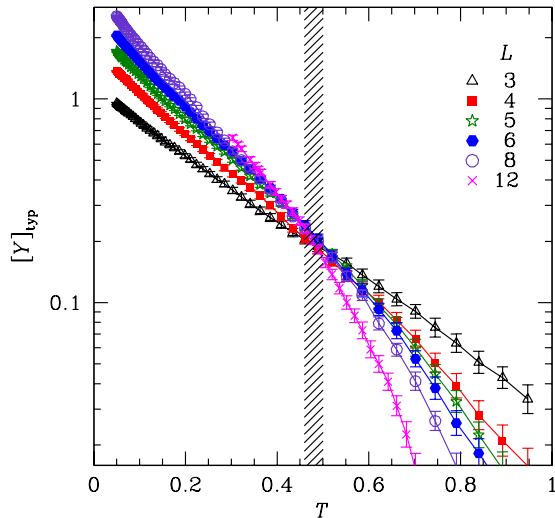


FIG. 6: (Color online) Typical (median) helicity modulus  $[Y]_{\text{typ}}$  as a function of temperature for different system sizes. The data are clearly nonzero in equilibrium and display the correct finite-size scaling; i.e., the data cross at  $T_c \approx 0.45 - 0.50$  (shaded area).

value of the transition temperature.

In order to improve on these results and properly account for the long tails in the distribution of the helicity modulus, we empirically fit the data for the distributions at different temperatures and system sizes to a generalized extreme-value distribution [Eq. (4)]; these are the solid lines in Figs. 3 and 4. The data are well represented by the fit, although in the tails the fitting routine slightly underestimates the tail at extremely low temperatures; however, this does not bias the results because the location parameter is mainly determined by the peak in the distribution.

We first study the shape of the helicity modulus distributions via the shape parameter  $\xi_Y$ . In Fig. 7, we show the shape parameter as a function of temperature for the different system sizes simulated. For  $T \gtrsim T_c$ , the shape parameter is negative for all  $L$ , thus indicating that when we are above the transition temperature the data are well described via a thin-tailed Weibull distribution. This is not the case for  $T \lesssim T_c$ , where the shape parameter increases for all system sizes when the temperature decreases to zero. In particular, already for small system sizes  $L \approx 8$  and  $T \approx 0.10$ , the shape parameter exceeds  $1/2$ ; i.e., the variance of the distribution is ill-defined. This explains the diverging fluctuations of the average helicity modulus in Fig. 5 for  $T \rightarrow 0$ . By extrapolating the data, we expect that for  $T \approx 0.10$  and  $L \gtrsim 15$ , the mean will not be properly defined any longer (since, then,  $\xi > 1$ ).

From a physical standpoint, a thin-tailed distribution for  $T > T_c$  suggests that vortex jumps, while they might occur, tend to be exponentially suppressed. This is not the case for  $T < T_c$ , where the tail of the distribution remains “fat;” i.e., arbitrarily large vortex rearrangements can occur. Note that for  $T \rightarrow \infty$ , we expect the distribution in the thermodynamic limit to become Gaussian, which corresponds to  $\xi = -1/2$ .

Because in an extreme-value distribution the location parameter  $\mu$  represents the most probable value (similar to the median), we show in Fig. 8 the location parameter of the helicity modulus distribution,  $\mu_Y$ , as a function of temperature for different system sizes. The data intersect cleanly at  $T = 0.48(2)$ , thus showing clear evidence of the glass transition. The fact that the data intersect so cleanly suggests that the helicity modulus distribution can be well described by extreme-value distributions. In the inset of Fig. 8, we show a finite-size scaling plot of the data according to

$$\mu_Y \sim \tilde{M}[L^{1/\nu}(T - T_c)], \quad (8)$$

where  $\tilde{M}$  is a scaling function and  $\nu$  is the critical exponent of the correlation length.<sup>38</sup> The best scaling collapse is determined by a nonlinear minimization routine<sup>39</sup> using the software package R.<sup>18,36</sup> The data scale well and we estimate  $T_c = 0.48(2)$  and  $\nu = 1.62(20)$ , in agreement with previous estimates of the critical exponents by Olson and Young computed from a finite-size scaling of the currents [ $T_c = 0.47(3)$  and  $\nu = 1.39(20)$ , see Ref. 11].<sup>40</sup> Note that a recently introduced extended scal-

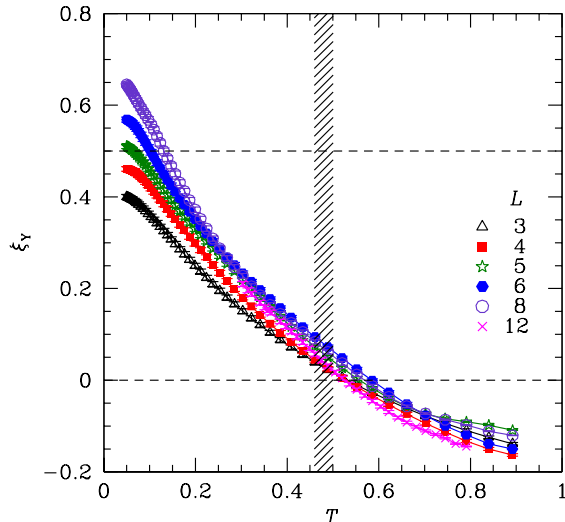


FIG. 7: (Color online) Shape parameter  $\xi_Y$  of the helicity modulus distribution as a function of temperature for different system sizes. Note that  $\xi_Y < 0$  for  $T \gtrsim T_c$  (shaded region); i.e., the distribution is thin-tailed and the moments of the distribution are properly defined. For  $T \lesssim T_c$ , the shape parameter is positive; i.e., the distribution is fat tailed. Already for  $T \approx 0.10$  and  $L \gtrsim 8$ , the standard deviation of the distribution is not properly defined ( $\xi_Y > 1/2$ , marked by the upper horizontal dashed line). This explains the strong fluctuations observed in the average helicity presented in Fig. 5.

ing scheme<sup>41</sup> might yield slightly different estimates for the critical exponents; however, we expect the location of the transition to remain unchanged.

Since the average helicity modulus is zero and the location parameter shows the correct critical behavior, we compute the superfluid density  $\rho_s^{\text{loc}}$  from Eq. (7) by replacing  $Y$  with  $\mu_Y$  and plot it as a function of system size  $L$  for different temperatures in Fig. 9. The data decay with increasing system size for all temperatures below and above the critical point and are well fitted by a phenomenological constant+exponential behavior, i.e.,  $\rho_s^{\text{loc}}(L) = a + b \exp(-cL)$  (dashed lines in Fig. 9) with fitting probabilities<sup>42</sup>  $Q \sim 0.3$  for  $T \rightarrow 0$ .<sup>43</sup> Therefore our results suggest that  $\rho_s^{\text{loc}}(L = \infty)$  is nonzero for the system sizes studied; for reference, Fisher *et al.* predict  $\rho_s^{\text{loc}} \sim a + b/\log(\omega/\omega_0)^x$  where  $\omega_0$  is a characteristic frequency and  $x$  an exponent, and Korshunov<sup>13</sup> predicts  $a = 0$ . We emphasize that our results do not rule out the scenario as predicted by Korshunov,<sup>13</sup> where the superfluid density is zero in equilibrium: The work of Korshunov is based on the existence of a hierarchical distribution of metastable states, and it is unclear if such an approximation would be valid for the gauge glass. In addition, large system sizes, which are numerically inaccessible, are required to probe a logarithmic behavior in detail.

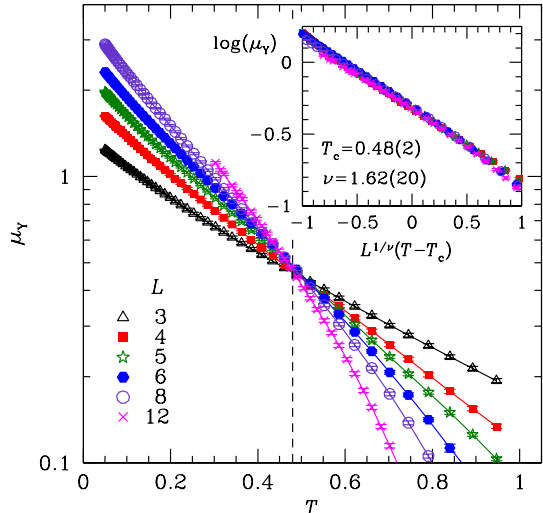


FIG. 8: (Color online) Location parameter of the helicity modulus distribution  $\mu_Y$  as a function of temperature for different system sizes. The data are nonzero and cross cleanly at  $T_c = 0.48(2)$ . The inset shows a finite-size scaling analysis of the data according to Eq. (8).  $L = 3$  has been omitted in the finite-size scaling analysis due to strong corrections to scaling. The observed scaling of the data suggests that generalized extreme-value distributions describe the helicity modulus distribution well. The vertical dashed line in the main panel at  $T = 0.48$  is a guide for the eyes.

The advantage of fitting the data with extreme-value distributions is also illustrated when studying the superfluid density: While the data for the typical estimate also display qualitatively the same behavior as the data computed from the location parameter, the fluctuations are considerably larger for the former (not shown) and fitting the data to extract any limiting behavior is impossible.

#### IV. CONCLUSIONS

We show that the distribution of the helicity modulus in the three-dimensional Gauge glass is well described by an extreme-value distribution and demonstrate that the typical value of the helicity modulus is nonzero, exhibiting critical scaling, whereas the behavior of the average value is an artifact of the boundary conditions: the average estimate is zero and displays strong fluctuations below the transition temperature. These fluctuations can be explained by fitting the data to an extreme-value distribution and by studying the shape parameter of the distribution. Below  $T_c$  the data are fat tailed, and thus, different moments of the distribution are ill defined.

In addition, we have computed the superfluid density from the location parameter of the extreme-value distribution and shown that it is finite in the thermody-

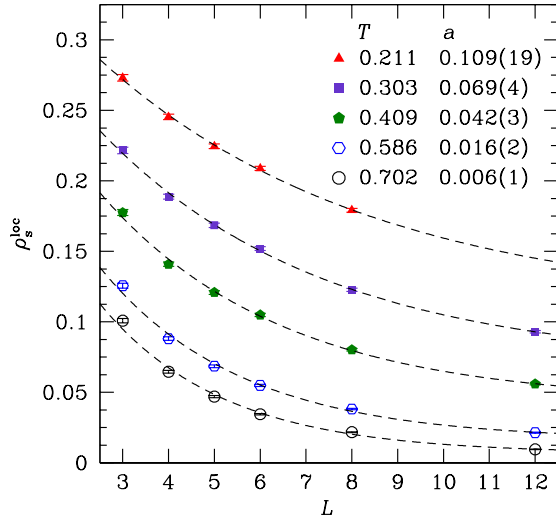


FIG. 9: (Color online) Superfluid density  $\rho_s^{\text{loc}}$  computed from the location parameter  $\mu_Y$  as a function of system size for different temperatures. The dashed lines are fits according to  $\rho_s^{\text{loc}}(L) = a + b \exp(-cL)$ .

dynamic limit. In this work, the equilibrium properties of the gauge glass [ $\omega \rightarrow 0$  limit before  $L \rightarrow \infty$  limit] have been studied. Another question of interest is if the limits  $L \rightarrow \infty$  and  $\omega \rightarrow 0$  are interchangeable. Assuming

the gauge glass to be a good effective model of the vortex glass phase in high-temperature superconductors, our results for the gauge glass imply that the superfluid density of the vortex glass is finite in the thermodynamic limit when the system is in equilibrium. Much larger system sizes are required to answer this question beyond reasonable doubt.

Finally, it might be of interest to perform similar studies on improved models of vortex glasses, such as the recently introduced model from Ref. 8 which includes the disorder via the couplings  $J_{ij}$  between the XY spins [see Eq. (1)]. Furthermore, the effects of screening on the gauge glass should be revisited at very low temperatures. We hope that this work will find application to other studies of observable distributions in physics where fat tails are involved.

### Acknowledgments

We would like to thank I. A. Campbell, V. B. Geshkenbein, H. Kawamura, S. E. Korshunov, M. Körner, Y. Ozeki, S. Trebst, M. Troyer, M. Wallin, G. T. Zimányi, and, in particular, A. P. Young for helpful discussions. H.G.K. thanks Heron Island for their hospitality during the last stages of the paper. The simulations were performed on the Asgard cluster at ETH Zürich. This work has been supported in part by the Swiss National Science Foundation.

- 
- <sup>1</sup> G. Blatter, M. V. Feigelman, V. B. Geshkenbein, A. I. Larkin, and V. M. Vinokur, *Vortices in high-temperature superconductors*, Rev. Mod. Phys. **66**, 1125 (1994).
  - <sup>2</sup> E. H. Brandt, *The flux-line lattice in superconductors*, Rep. Prog. Phys. **58**, 1465 (1995).
  - <sup>3</sup> T. Nattermann and S. Scheidl, *Vortex-glass phases in type-II superconductors*, Adv. Phys. **49**, 607 (2000).
  - <sup>4</sup> G. Blatter and V. B. Geshkenbein, *Vortex matter*, in *The Physics of Superconductors, Vol. 1, Conventional and High- $T_c$  superconductors*, edited by K. H. Bennemann and J. B. Ketterson (Springer, Berlin, 2003), p. 726.
  - <sup>5</sup> Note that high-temperature superconductors also possess an intrinsic material anisotropy which can be rescaled away (Ref. 1).
  - <sup>6</sup> C. Wengel and A. P. Young, *Monte Carlo study of a three-dimensional vortex-glass model with screening*, Phys. Rev. B **54**, R6869 (1996).
  - <sup>7</sup> B. I. Spivak and S. A. Kivelson, *Negative local superfluid densities: The difference between dirty superconductors and dirty Bose liquids*, Phys. Rev. B **43**, 3740 (1991).
  - <sup>8</sup> H. Kawamura, *Simulation studies on the stability of the vortex-glass order*, J. Phys. Soc. Jpn. **69**, 29 (2000).
  - <sup>9</sup> T. Giamarchi and P. Le Doussal, *Elastic theory of pinned flux lattices*, Phys. Rev. Lett. **72**, 1530 (1994).
  - <sup>10</sup> P. G. de Gennes, *Superconductivity of Metals and Alloys* (Addison-Wesley, Redwood City, 1989).
  - <sup>11</sup> T. Olson and A. P. Young, *Finite temperature ordering in the three-dimensional gauge glass*, Phys. Rev. B **61**, 12467 (2000).
  - <sup>12</sup> D. S. Fisher, M. P. A. Fisher, and D. A. Huse, *Thermal fluctuations, quenched disorder, phase transitions, and transport in type-II superconductors*, Phys. Rev. B. **43**, 130 (1991).
  - <sup>13</sup> S. E. Korshunov, *Low-frequency response of a collectively pinned vortex manifold*, Phys. Rev. B **63**, 174514 (2001).
  - <sup>14</sup> W. M. Saslow, M. Gabay, and W.-M. Zhang, *“Spiraling” algorithm: Collective Monte Carlo trial and self-determined boundary conditions for incommensurate spin systems*, Phys. Rev. Lett. **68**, 3627 (1992).
  - <sup>15</sup> P. Olsson, *Monte Carlo analysis of the two-dimensional XY model. II. Comparison with the Kosterlitz renormalization-group equations*, Phys. Rev. B **52**, 4526 (1995).
  - <sup>16</sup> E. J. Gumbel, *Statistics of Extremes* (Columbia University Press, New York, 1958).
  - <sup>17</sup> E. J. Gumbel, *Multivariate Extremal Distributions*, Bull. Inst. Internat. de Statistique **37**, 471 (1960).
  - <sup>18</sup> Rmetrics Core Team, URL <http://www.rmetrics.org>.
  - <sup>19</sup> M. P. A. Fisher, *Vortex-glass superconductivity: A possible new phase in bulk high- $T_c$  oxides*, Phys. Rev. Lett. **62**, 1415 (1989).
  - <sup>20</sup> K. Binder and A. P. Young, *Spin glasses: Experimental*

- facts, theoretical concepts and open questions, *Rev. Mod. Phys.* **58**, 801 (1986).
- <sup>21</sup> R. H. Koch, V. Foglietti, W. J. Gallagher, G. Koren, A. Gupta, and M. Fisher, *Experimental evidence for vortex-glass superconductivity in Y-Ba-Cu-O*, *Phys. Rev. Lett.* **63**, 1511 (1989).
- <sup>22</sup> P. L. Gammel, L. F. Schneemeyer, and D. J. Bishop, *SQUID picovoltometry of YBa<sub>2</sub>Cu<sub>3</sub>O<sub>7</sub> single crystals - Evidence for a finite-temperature phase transition in the high-field vortex state*, *Phys. Rev. Lett.* **66**, 953 (1991).
- <sup>23</sup> H. K. Olsson, R. H. Koch, W. Eidelloth, and R. P. Rober-tazzi, *Observation of critical scaling behavior in the ac impedance at the onset of superconductivity in a large mag-netic field*, *Phys. Rev. Lett.* **66**, 2661 (1991).
- <sup>24</sup> U. Divakar, A. J. Drew, S. L. Lee, R. Gilardi, J. Mesot, F. Y. Ogrin, D. Charalambous, E. M. Forgan, G. I. Menon, N. Momono, et al., *Direct Observation of the Flux-Line Vortex Glass Phase in a Type II Superconductor*, *Phys. Rev. Lett.* **92**, 237004 (2004).
- <sup>25</sup> H. G. Katzgraber and A. P. Young, *Nature of the spin-glass state in the three-dimensional gauge glass*, *Phys. Rev. B* **64**, 104426 (2001).
- <sup>26</sup> J. D. Reger, T. A. Tokuyasu, A. P. Young, and M. P. A. Fisher, *Vortex-glass transition in three dimensions*, *Phys. Rev. B* **44**, 7147 (1991).
- <sup>27</sup> A twist along the  $y$  and  $z$  directions would yield the same results.
- <sup>28</sup> P. Dayal, S. Trebst, S. Wessel, D. Würtz, M. Troyer, S. Sabhapandit, and S. N. Coppersmith, *Performance Lim-itations of Flat-Histogram Methods*, *Phys. Rev. Lett.* **92**, 097201 (2004).
- <sup>29</sup> S. Alder, S. Trebst, A. K. Hartmann, and M. Troyer, *Dy-namics of the Wang Landau algorithm and complexity of rare events for the three-dimensional bimodal Ising spin glass*, *J. Stat. Mech.* P07008 (2004).
- <sup>30</sup> E. Bertin and M. Clusel, *Generalised extreme value statis-tics and sum of correlated variables*, *J. Phys. A* **39**, 7607 (2006).
- <sup>31</sup> K. Hukushima and K. Nemoto, *Exchange Monte Carlo method and application to spin glass simulations*, *J. Phys. Soc. Jpn.* **65**, 1604 (1996).
- <sup>32</sup> E. Marinari, *Optimized Monte Carlo methods*, in *Ad-vances in Computer Simulation*, edited by J. Kertész and I. Kondor (Springer-Verlag, Berlin, 1998), p. 50, (cond-mat/9612010).
- <sup>33</sup> H. G. Katzgraber and A. P. Young, *Numerical studies of the two- and three-dimensional gauge glass at low temper-ature*, *Phys. Rev. B* **66**, 224507 (2002).
- <sup>34</sup> For  $L \leq 8$  we use the same simulation parameters as in Ref. 25 where a thorough equilibration test was performed.
- <sup>35</sup> M. Cieplak, J. R. Banavar, M. S. Li, and A. Khurana, *Frustration, scaling, and local gauge invariance*, *Phys. Rev. B* **45**, 786 (1992).
- <sup>36</sup> R Core Team, URL <http://cran.r-project.org>.
- <sup>37</sup> Temperatures used in the simulation: 0.050, 0.052, 0.054, 0.056, 0.058, 0.060, 0.062, 0.066, 0.069, 0.072, 0.076, 0.081, 0.086, 0.091, 0.097, 0.103, 0.109, 0.116, 0.123, 0.131, 0.139, 0.147, 0.156, 0.166, 0.176, 0.187, 0.199, 0.211, 0.224, 0.238, 0.253, 0.269, 0.285, 0.303, 0.322, 0.341, 0.363, 0.385, 0.409, 0.434, 0.461, 0.489, 0.520, 0.552, 0.586, 0.622, 0.661, 0.702, 0.745, 0.791, 0.840, 0.892, 0.947.
- <sup>38</sup> J. M. Yeomans, *Statistical Mechanics of Phase Transitions* (Oxford University Press, Oxford, 1992).
- <sup>39</sup> H. G. Katzgraber, M. Körner, and A. P. Young, *Universal-ity in three-dimensional Ising spin glasses: A Monte Carlo study*, *Phys. Rev. B* **73**, 224432 (2006).
- <sup>40</sup> In two space dimensions the gauge glass does not have a transition at finite temperatures (see Refs. 44 and 45). We have also computed the helicity modulus distribution of the two-dimensional gauge glass. Unpublished data for the location parameter of the helicity modulus distribution supports a zero-temperature transition.
- <sup>41</sup> I. A. Campbell, K. Hukushima, and H. Takayama, *An Ex-tended Scaling Scheme for Critically Divergent Quantities*, *Phys. Rev. Lett.* **97**, 117202 (2006).
- <sup>42</sup> W. H. Press, S. A. Teukolsky, W. T. Vetterling, and B. P. Flannery, *Numerical Recipes in C* (Cambridge University Press, Cambridge, 1995).
- <sup>43</sup> We have also tried other fitting functions inspired by the results of Ref. 19, i.e.,  $\rho_s^{\text{loc}} \sim a + [\tilde{b}/\log(L/L_0)]^x$  where  $L_0$  is a characteristic length scale and  $x$  an exponent. In the previous expression we have assumed a power-law relation-ship between the driving frequency  $\omega$  and the system size  $L$ , i.e.,  $\omega \sim L^{-z}$ . Unfortunately, attempting to fit the nu-merical data to the aforementioned functional form yielded extremely poor fitting probabilities ( $Q \sim 10^{-6}$ ).
- <sup>44</sup> H. Nishimori and H. Kawamura, *Gauge Glass Ordering in Two Dimensions*, *J. Phys. Soc. Jpn.* **62**, 3266 (1993).
- <sup>45</sup> H. G. Katzgraber, *On the existence of a finite-temperature transition in the two-dimensional gauge glass*, *Phys. Rev. B* **67**, 180402(R) (2003).